NEIGHBORTRACK: IMPROVING SINGLE OBJECT TRACKING BY BIPARTITE MATCHING WITH NEIGHBOR TRACKLETS

A PREPRINT

Yu-Hsi Chen¹, Chien-Yao Wang¹, Cheng-Yun Yang², Hung-Shuo Chang¹, Youn-Long Lin³, Yung-Yu Chuang⁴, and Hong-Yuan Mark Liao¹

¹Institute of Information Science, Academia Sinica, Taiwan, {franktpmvu,kinyiu,jonathanc,liao}@iis.sinica.edu.tw
²Department of Electrical Engineering, Purdue University, yang2316@purdue.edu
³Department of Computer Science, National Tsing Hua University, ylin@cs.nthu.edu.tw
⁴Department of Computer Science and Information Engineering, National Taiwan University, lcyy@csie.ntu.edu.tw

April 14, 2023

ABSTRACT

We propose a post-processor, called NeighborTrack, that leverages neighbor information of the tracking target to validate and improve single-object tracking (SOT) results. It requires no additional data or retraining. Instead, it uses the confidence score predicted by the backbone SOT network to automatically derive neighbor information and then uses this information to improve the tracking results. When tracking an occluded target, its appearance features are untrustworthy. However, a general siamese network often cannot tell whether the tracked object is occluded by reading the confidence score alone, because it could be misled by neighbors with high confidence scores. Our proposed NeighborTrack takes advantage of unoccluded neighbors' information to reconfirm the tracking target and reduces false tracking when the target is occluded. For the VOT challenge dataset commonly used in short-term object tracking, we improve three famous SOT networks, Ocean, TransT, and OSTrack, by an average of 1.92% EAO and 2.11% robustness. For the mid- and long-term tracking experiments based on OSTrack, we achieve state-of-the-art 72.25% AUC on LaSOT and 75.7% AO on GOT-10K. Code duplication can be found in https://github.com/franktpmvu/NeighborTrack.

1 Introduction

Single Object Tracking (SOT) is a fundamental computer vision task that establishes the correspondence of an arbitrarily specified object along time [24]. There are numerous applications for it, including video surveillance [19, 27], video annotation [1], human-computer interaction [18], etc. An SOT network takes a user-specified target of interest in the first frame and then tracks its position in subsequent frames. In contrast to multi-object tracking (MOT), which knows the target classes in advance, SOT is unaware of the target classes. The current SOT approaches use various algorithms derived from the Siamese network [2]. With the help of a deep learning network, they extract the appearance feature of the target object and then use that feature to locate the positions of objects with similar features in subsequent frames. Using pairwise appearance feature alignment, the same network can be used to track multiple objects with different appearance features without requiring retraining. This approach, however, might fail to track when the appearance characteristics of either side change.

In recent years, deep neural network-based feature extraction has led to an increase in the accuracy of tracking objects. It is, however, unreliable to track objects purely based on their appearance features, as their appearance can change due to deformations, changes in size, changes in color, and occlusions. In particular, occlusion presents a serious challenge since we cannot predict what objects are occluding the target or are occluded by the target, and therefore cannot use the partial appearance to continue tracking. Further, when tracking one among several similar objects, occlusion may cause the tracker to assume an incorrect position.

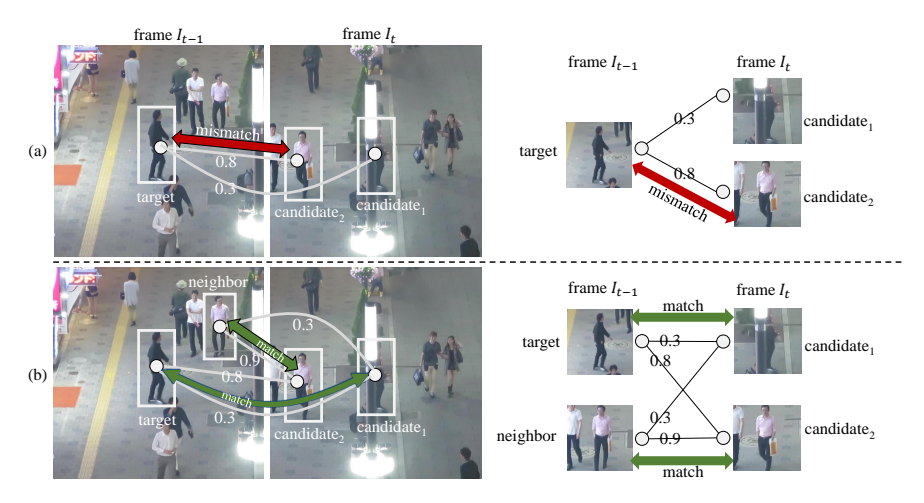


Figure 1: An illustrative example of how neighbor information can be used to correct tracking results. Neighbor are objects that are similar to the target in the track space (visually or spatiotemporally) and are the major source of false matches to the target. (a) Tracking without considering neighbors. As shown in the graph on the right, the association problem can be viewed as a bipartite matching problem between candidates and the target. The edge weight is the similarity. Matching between the target alone and candidates can be unreliable when there is occlusion. As shown in this example, the target is incorrectly matched with candidate₂ since it has a lower similarity to the correct match (candidate₁) as a result of occlusion. (b) Tracking with considering neighbors. In this example, since the neighbor is not occluded, it can be matched with candidate₂ correctly. As a result, the target must match candidate₁, since matching the same candidate is not permitted. The matching procedure can be formulated as a bipartite matching problem between candidates and the target along with neighbors. It can be seen, in this example, that by including neighbors in the matching process, the accuracy of matching and tracking can be improved. (The example is from MOT16 [21].)

To address the challenges caused by appearance changes, we propose a post-processor named NeighborTrack. The main idea is to verify the correctness of the tracking result using the spatial-temporal trajectories of the neighbors of the target. NeighborTrack simultaneously tracks the target and its neighbors. When the target is occluded, it reduces the number of matching errors by involving neighbors in the matching process.

Consider the example in Figure 1. In the current frame I_t , there are two candidates for the tracking target. Numbers on the edges indicate the similarity between two objects. In frame I_t , the target object is occluded. When only considering appearance cues (Figure 1(a)), the target is incorrectly matched to the wrong candidate₂ because of occlusion. Aside from visual and spatiotemporal cues, NeighborTrack makes use of neighbors in the previous frame in order to resolve ambiguities caused by occlusions. Neighbors are objects that are similar to the target object. Often, they are the source of ambiguity. By considering neighbors (Figure 1(b)), we construct a bipartite graph with two sets of nodes: one for the hypothesis of matches (candidates) and one for the source of ambiguity (neighbors) and the target. After bipartite matching, since the neighbor is not occluded, it can be correctly matched with candidate₂. The target should therefore choose candidate₁ (the correct one), even if their similarity remains low due to occlusions. Note that NeighborTrack uses the spatial-temporal tracklets of the neighbors for more robust similarity estimation. Our experiments indicate that NeighborTrack effectively mitigates the problems caused by occlusion and increases tracking accuracy.

We propose NeighborTrack, a post-processor for improving SOT, and have made the following contributions.

- We formulate the association problem as a bipartite matching problem between candidate and neighbor tracklets. Unlike attention-based methods that strengthen single-target appearance features, our method uses neighbor information to help correct wrong tracking when appearance features change.
- Based on cycle consistency, we calculate Intersection over Union (IoU) between two tracklets as a more robust measure of similarity. Both spatiotemporal and visual cues are considered in the measurement.
- Our approach is not in conflict with, and it can complement, methods for enhancing appearance features or enhancing object localization, such as DIMP [3] and the Alpha-refine [30]. The agnostic nature of our method enables it to be combined with most SOT methods.
- Our method does not require additional training data or retraining or fine-tuning, and neighbor information is readily available from the network-generated confidence scores without additional computation.

• We achieved state-of-the-art 72.25% AUC on the LaSOT [8] dataset. For the GOT-10K[10] dataset, we achieved 75.7% AO. On the bbox and mask datasets of VOT challenge [13], our method increases EAO and robustness by 2.11% and 1.92%, respectively.

2 Related Work

SOT methods based on Siamese networks [2] have been continuously refined and improved. The majority of research has focused on improving the header function by adding more effective tracking mechanisms. Some methods [15, 16] borrow the region proposal network mechanism from Faster R-CNNs [23] to make a network more adaptive to target size changes. Wang et al. [24] propose a method that generates a mask for tracking the target while training the tracker in order to enable the network to track targets more accurately and interpretably when used in real scenes. Ocean [33] replaces anchor-based headers with anchor-free ones to alleviate issues associated with overlapping tracked targets and anchors in a crowded scene. Aside from the header issue, effective extraction of appearance features has always been a focus of SOT research. Recent methods [5, 6, 31] achieve breakthrough performance by employing a transformer network to simultaneously track the target and all the surrounding backgrounds, and then establishing an appearance feature model covering both self-attention and cross-attention.

Although the above-mentioned methods improve object tracking, they cannot overcome the tracking difficulties caused by occlusion [14]. Siamese network-based methods often fail when appearances change; therefore, relying solely on appearances is not unreliable. The confidence score predicted by a siamese network is a good indicator of appearance similarity, and objects with a similar appearance to the target will have high confidence scores. According to the tracking results on VOT challenge [13] reported by Zhang et al. [33], when non-tracking objects occlude the target object, the target appearance will change significantly, and this will greatly reduce the confidence score of the target position. It is therefore necessary to consider other information to overcome the challenge of occlusion.

The use of neighboring information is common in most multi-object tracking (MOT) systems. Even though the MOT task must consider multiple-to-multiple tracking, it is actually equivalent to taking into account the time-space matching relationship of all objects in the search range at the same time. There are, however, two differences between SOT and MOT. (1) Most MOT networks such as FairMOT [32] only track certain pre-determined classes. In contrast, a general SOT system should be able to track virtually any type of object. The feature space of an MOT model can be pre-trained on a class-specific Re-ID task to distinguish objects within a class, which is not applicable to objects outside the class. To be more specific, MOT has a considerable degree of pertinence in extracting appearance features. Targets will not be significantly affected by appearance features as long as their key parts are not occluded. As for SOT, it does not have the above class information, and the requirements for appearance characteristics must be universal. Therefore, it is more susceptible to occlusion problems. (2) In the design of an MOT system, objects of the same class are tracked together. This is actually beneficial to tracking because the matching relationship between multiple objects and the background or other objects can be easily defined and then used to correct the tracking results. As for SOT, it does not have direct access to information about object adjacency. In DIMP [3], the authors propose to learn foreground/background information directly so as to adapt to different backgrounds in different videos. But, this approach essentially only considers the appearance characteristics of a single target, as opposed to an MOT system which directly uses the matching relationship between multiple objects. Due to the nature of the SOT task, it is not possible to predict in advance the information regarding class and Re-ID. This paper presents a systematic approach to utilizing neighbor information for SOT.

Some methods [34, 20] take into account multiple objects in the SOT task. DMTrack [34] adds a Re-ID network without class information to the SOT task; however, it should be noted that the Re-ID feature cannot be easily generalized to data that have not yet been trained before [7]. KeepTrack [20] trains a graph neural network to determine the tracking result after referring to all candidate regions in two adjacent frames. In comparison with these methods that utilize information across objects or frames, our method offers the following advantages: (1) Our method is a post-processing method. Thus, unlike these methods, our method does not require an additional network and retraining to obtain neighbor information, making it more flexible to use. (2) These methods only take into account information from two adjacent frames. Whenever a target is occluded, at least one frame's target appearance features will be unreliable. As a result of incorporating past information for a period of time, our method is able to better reduce tracking inaccuracies resulting from occlusions or changes in appearance over time.

3 NeighborTrack

This paper proposes NeighborTrack for improving the tracking results of an SOT network Φ as long as it meets two requirements. First, given a target template patch z, its bounding box b_0 specifying its position at the first frame I_0 , and

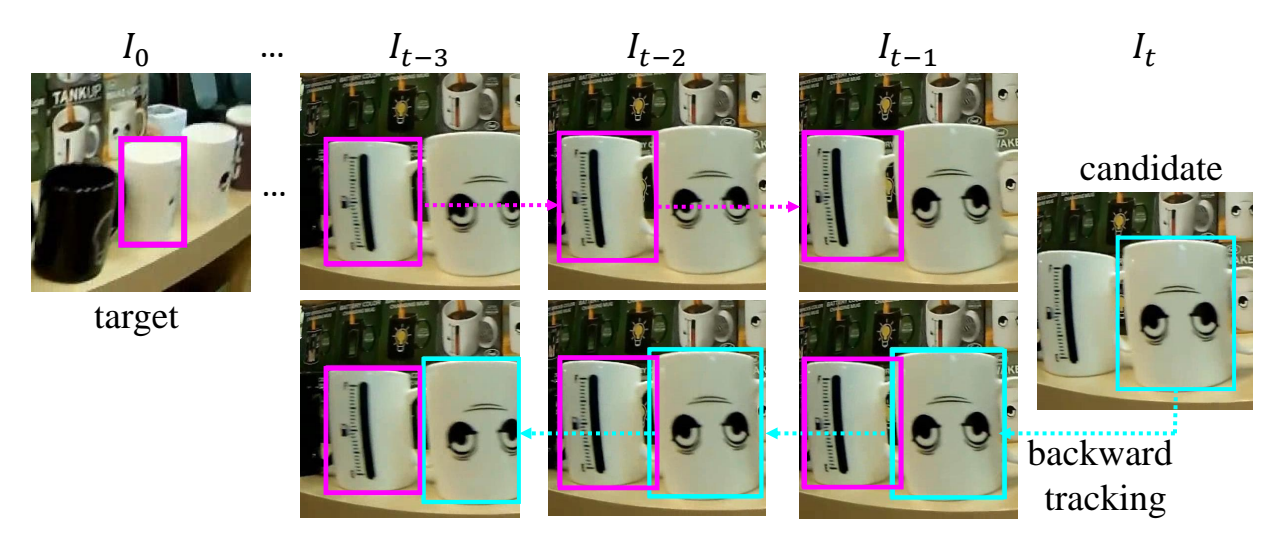


Figure 2: A real example of using cycle consistency to eliminate incorrect candidates The example is from LaSOT [8]. Based on the target template at I_0 , the tracker (OSTrack [31] in this example) tracks it until the frame I_{t-1} and produces a target tracklet (magenta boxes). For the current frame I_t , it selects the incorrect candidate due to severe view changes from the template. As a result of backtracking the candidate, we are able to obtain its backward-tracking candidate tracklet (cyan boxes). After calculating its similarity to the forward-tracking target tracklet, it is clear that the candidate does not match the target well. Using the proposed measure, we are able to verify matches better by utilizing the spatiotemporal relationship.

a sequence of frames (I_1, \dots, I_T) , the network Φ can generate a tracking result (b_1, \dots, b_T) where b_t is the bounding box indicating the position of the target object at frame I_t . Second, for a frame I_t , the network can generate a set of candidate bounding boxes B^t and their confidence scores S^t . The two requirements are met by the majority of SOT networks.

To determine the bounding box of the target object at the current frame I_t , NeighborTrack produces a set of candidate bounding boxes \mathcal{C}^t . These are the hypotheses that the target matches. Among the candidates, we are seeking to identify the best match for the target. To have a more robust similarity measurement, NeighborTrack is inspired by the principle of cycle consistency [25]: an object tracked forward along a time line should be able to return to its original position when tracked backwards along time. In the current frame I_t , we have a forward-tracking tracklet $(b_{t-\tau}, \cdots, b_{t-1})$ for the target object. For the purpose of utilizing cycle consistency for similarity, we backtrack each candidate using Φ for τ frames in order to extract its backward-tracking tracklet. A candidate tracklet pool \mathbf{P}^c is formed by these tracklets. Similarity between two tracklets is determined by their intersection over union (IoU) value. The measurement considers both visual and spatiotemporal cues since IoU takes the spatiotemporal cue into account, while visual cues are considered when tracklets are formed through forward/backward tracking. By measuring the similarity between the forward-tracking target tracklet and the backward-tracking candidate tracklet, we can verify how closely a candidate matches the target object using forward/backward tracking and cycle consistency. Figure 2 illustrates a real example of how a tracker can eliminate incorrect matches by ensuring cycle consistency.

NeighborTrack also maintains a neighbor tracklet pool \mathbf{P}^n which contains neighbors that are similar to the target. Since neighbors are similar to the target (visually and spatiotemporally), they can cause false matches, particularly when the target's appearance changes or when it is obscured. As illustrated in Section 1, the neighbors are used to resolve ambiguity.

3.1 Candidate and neighbor tracklets

Candidate set. As one of the requirements, given the previous tracking results (b_1,\cdots,b_{t-1}) for (I_1,\cdots,I_{t-1}) , the SOT network can generate a list of n_t candidate bounding boxes $\tilde{B}^t = \{\tilde{b}_1^t,\cdots,\tilde{b}_{n_t}^t\}$ and their corresponding confidence scores $\tilde{S}^t = \{\tilde{s}_1^t,\cdots,\tilde{s}_{n_t}^t\}$ for the current frame I_t . Most SOT methods find the bounding box $\tilde{b}_{i_{max}}^t$ with the highest confidence score as the tracking result of I_t , where $i_{max} = \arg\max_i \tilde{s}_i^t$. Instead of picking up the most confident one, NeighborTrack maintains a candidate set of bounding boxes \mathcal{C}^t and finds the match within \mathcal{C}^t . We first

filter out bounding boxes with insufficient confidence scores:

$$(\hat{B}^t, \hat{S}^t) = \{(\tilde{b}_i^t, \tilde{s}_i^t) \mid \tilde{b}_i^t \in \tilde{B}^t \text{ and } \tilde{s}_i^t > \alpha \tilde{s}_{i_{max}}^t)\}, \tag{1}$$

where $\alpha \in [0,1]$ is a hyperparameter for the threshold confidence ratio, \hat{B}^t is the set of candidate bounding boxes with sufficient confidence and \hat{S}^t are their confidence scores. Next, we perform non-maximum suppression on the remaining bounding boxes:

$$(B^t, S^t) = \text{SoftNMS}(\hat{B}^t, \hat{S}^t), \tag{2}$$

where SoftNMS is an improved version of non-maximum suppression [4], B^t and S^t respectively contain the bounding boxes and adjusted scores after SoftNMS.

If the target object is severely occluded, the correct match may not be included in the candidate set even if a loose threshold is applied. Thus, we also apply a Kalman filter to predict the candidate bounding box b^{κ} without relying on appearance features. The candidate set \mathcal{C}^t is formed by adding b^{κ} into B^t , i.e., $\mathcal{C}^t = B^t \cup \{b^{\kappa}\}$.

Candidate tracklet pool. For each candidate $b_i^t \in \mathcal{C}^t$, we generate its tracklet ξ_i^t by backtracking for τ frames. We set the patch z_i^t as the target template which is the patch cropped from using the bounding box b_i^t and use the SOT network Φ for backtracking, i.e.,

$$\xi_i^t = \Phi(z_i^t, b_i^t, (I_{t-1}, \cdots, I_{t-\tau})). \tag{3}$$

The tracklet ξ_i^t is a sequence of bounding boxes indicating the positions of the target template z_i^t from time t-1 to time t-1. The set of all candidate tracklets is referred to as the candidate tracklet pool \mathbf{P}^c . Intuitively, the candidate tracklet pool contains the backtracking tracklets of objects that could potentially be the target object.

Neighbor tracklet pool. NeighborTrack also maintains another tracklet pool called the neighbor pool \mathbf{P}^n . Neighbor tracklets are essentially the candidate tracklets from the previous frame. By applying the method described in section Section 3.2, NeighborTrack selects a bounding box b_m^t in the candidate set \mathcal{C}^t as the tracking result for I_t . Afterwards, NeighborTrack updates the neighbor pool \mathbf{P}^n using the current candidate tracklet pool \mathbf{P}^c . In the first step, the selected tracklet ξ_m^t is removed from \mathbf{P}^c . For each tracklet ξ_i^t remaining in \mathbf{P}^c , we adjust its time span from $[t-1,t-\tau]$ to $[t,t-\tau+1]$ to be ready for the next frame I_{t+1} . This is accomplished by appending the associate candidate bounding box b_i^t at the head and removing the last bounding box:

$$\zeta_i^{t+1} = (b_i^t) \hat{\rho}(\xi_i^t), \tag{4}$$

where \cap is the concatenation operator of two sequences and $\rho(s)$ removes the last element from the sequence s. The neighbor tracklet \mathbf{P}^n is updated by $\{\zeta_i^{t+1}|i\neq m\}$ for the next frame I_{t+1} . As a result, the neighbor tracklets are the unselected candidate tracklets from the previous frame (after aligning the time span to the current frame).

We maintain the neighbor tracklets because they belong to neighbors of the target object in the tracking space. They are similar to the target object either visually or spatiotemporally and may cause ambiguity to the SOT network, particularly when the target object is obscured. By bipartite matching with those neighbors (Section 3.2), the ambiguity could be better resolved.

We only retain neighbor tracklets from the previous frame, not those from earlier frames. There are several reasons for this. To begin with, tracking accuracy degrades over time as outdated neighbor tracklets rarely provide useful information. Additionally, if a neighbor tracklet continues to survive, it should be possible to find the correspondence at the most recent time. Finally, retaining more tracklets will increase computation overhead. Thus, to avoid filling the pool with outdated neighbor tracklets that slow down computation speed, we only retain candidate tracklets from the previous time instance.

3.2 Tracking by bipartite matching

Through the process introduced in Section 3.1, we have the candidate pool \mathbf{P}^c and the neighbor pool \mathbf{P}^n . The candidate pool contains hypothesis of tracking results while the neighbor pool contains the source of potential ambiguity. Given the target tracklet $\eta = (b_{t-1}, \cdots, b_{t-\tau})$ which is the tracking results for the previous τ frames, our goal is to find the association of η among hypothesis \mathbf{P}^c while verifying with the source of ambiguity \mathbf{P}^n .

We cast the association problem into a bipartite matching problem. We have two sets of tracklets: $\mathbf{S}^c = \mathbf{P}^c$ and $\mathbf{S}^n = \mathbf{P}^n \cup \{\eta\}$. Each tracklet in \mathbf{S}^c and \mathbf{S}^n can be taken as a node. Thus, we have a bipartite graph whose two independent sets of nodes formed by \mathbf{S}^c and \mathbf{S}^n . It is a complete bipartite graph since every node of the first set \mathbf{S}^c is connected to every node of the second set \mathbf{S}^n . The weight w_{ij} associated with the edge between two nodes,

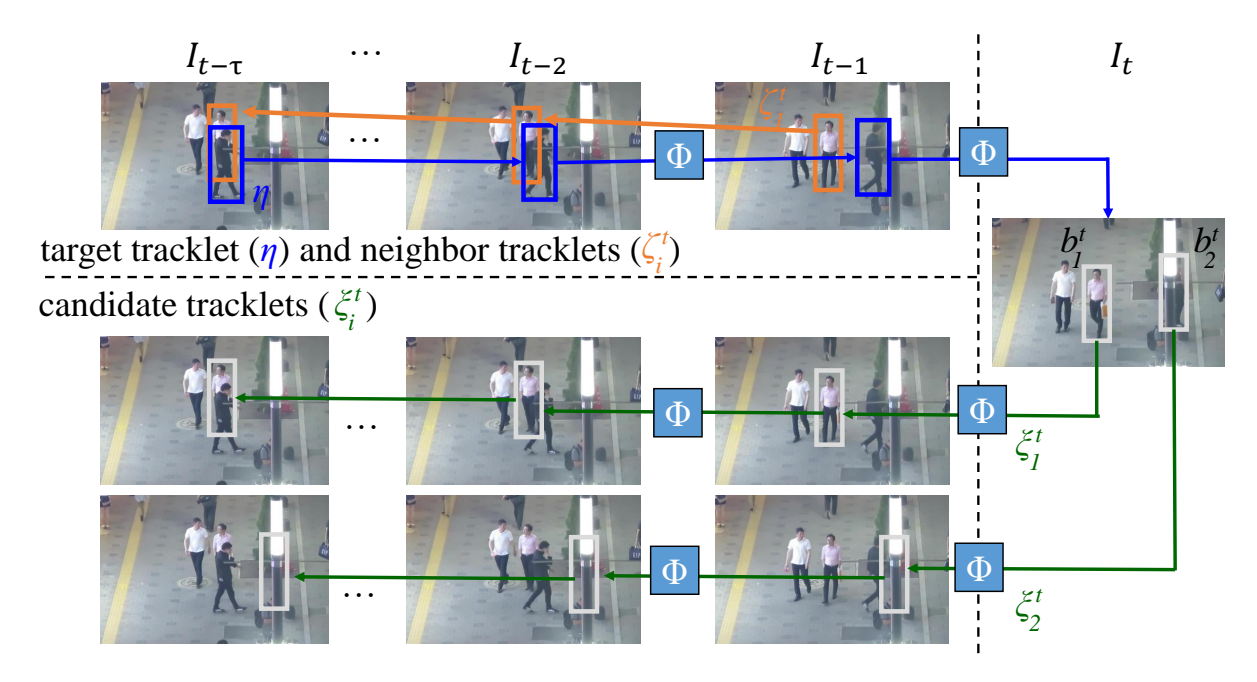


Figure 3: An illustration of the candidate and neighbor tracklets. The blue boxes represent the target tracklet (η) , while the orange boxes represent a neighbor tracklet (ζ_1^t) . For the current frame I_t , the tracker Φ generates a set of candidates (the white boxes), b_1^t and b_2^t , in I_t . Using Φ for backtracking, we obtain their candidate tracklets (ξ_1^t) and ξ_2^t . Note that since the target object is occluded in I_t , the confidence score of the correct candidate (b_2^t) is lower than that of the incorrect candidate (b_1^t) . However, as b_1^t 's candidate tracklet (ξ_1^t) matches very well with the neighbor tracklet (ζ_1^t) , bipartite matching decides to match it with the neighbor rather than the target. Therefore, the target η has to be matched with the candidate ξ_2^t , thus correcting the false tracking. The example is from MOT16 [21].

 $\xi_i^t \in \mathbf{S}^c$ and $\zeta_j^t \in \mathbf{S}^n$, is defined as the average IoU values between two tracklets. That is, if $\xi_i^t = (b_{t-1}^c, \cdots, b_{t-\tau}^c)$ and $\zeta_j^t = (b_{t-1}^n, \cdots, b_{t-\tau}^n)$, then we have

$$w_{ij} = \frac{1}{\tau} \sum_{k=t-\tau}^{t-1} \text{IoU}(b_k^c, b_k^n),$$
 (5)

where IoU calculates the IoU values between two bounding boxes. The weight reflects the trajectory similarity between two tracklets. We employ the Hungarian algorithm [22] to find the maximum matching for the resultant bipartite graph. Suppose that the candidate tracklet ξ_m^t is paired with the target tracklet η , its corresponding candidate bounding box b_m^t is selected as the tracking result for frame I_t . When the target tracklet η is not matched, we select the non-matched candidate tracklet with the highest IoU values with η . If the highest IoU is zero, we select the candidate b^κ predicted by the Kalman filter.

It is important to note that, although we only take the match of the target tracklet as the tracking result, all neighboring tracklets serve as a means of verifying the tracking result. If a candidate tracklet has a high IoU similarity to the target tracklet, it is likely to be the target. In contrast, if it has a high IoU similarity with any neighbor tracklet, it is likely to be associated with another object rather than the target. In this way, neighbor tracklets contribute to the matching process and assist in resolving ambiguities.

Tracking is significantly hampered by occlusions. Since the appearance feature is unreliable, it is easy to lose track of a target that has been occluded in the current frame. NeighborTrack addresses this issue with the help of neighbor tracklets. Assuming that the target object is occluded in the current frame, the correct candidate tracklet will have a lower similarity to the target tracklet. However, NeighborTrack can still find the correct tracking result as long as the objects in the candidate set are not occluded. Since the candidate objects are not occluded, their candidate tracklets can find excellent matches among the neighbor tracklets and will not select the target tracklet as their matches. Figure 3 gives an example on how bipartite matching works.

Our edge weight only considers the similarity of bounding boxes, and not the visual similarity of patches. There are two reasons for this. First of all, the appearance feature of an occluded target is less unreliable. In the event that the target is occluded, its appearance may resemble that of the occluder. Thus, visual similarity could mislead the results.

Secondly, we construct candidate tracklets by backtracking patches of the candidate objects. In this way, the appearance features of candidates have already been implicitly considered in the tracklets.

4 Experiments

We begin by discussing the details of implementation in this section. Then, we apply NeighborTrack to improve several SOT networks and report the results on the VOT [13], LaSOT [8] and GOT-10K [10] datasets.

4.1 Implementation details

We used the following parameters in all experiments. A threshold ratio of $\alpha=0.7$ is used to select candidate bounding boxes. For SoftNMS [4], the IoU threshold is set to 0.25, and σ is set to 0.01 for the Gaussian penalty function. The time period τ of backtracking tracklets is 9. In order to maintain neighbor information and enforce bipartite matching, our method slightly lowers the frame rate, as shown in Table 1. The hardware used in the experiment is 8 GTX 1080TI and 2 Intel E5 2620v4 CPU. When the time period τ is equal to 9, the frame rate is 43% of the baseline. Also, not including Kalman filter will slightly reduce the performance of our method $(0.722 \to 0.720)$ when setting the same τ . As for the frame rate, it will increase slightly $(1.58 \to 1.71)$ due to the number decrease of the neighbors.

Because NeighborTrack requires extra computation, it is only activated when tracking results become unstable. We consider tracking results stable and will not activate NeighborTrack if two conditions are met. (1) If there is only one candidate in the set \mathcal{C}^t , there is no other option to match except $b^t_{i_{max}}$. (2) If the average IoU between the target tracklet η and the most confident candidate tracklet $\xi^t_{i_{max}}$ is higher than a threshold, then the tracking result is stable.

4.2 Datasets and competing methods

We conduct experiments on both short-term and long-term tracking. For short-term tracking, we use the VOT challenge [13] datasets including VOT2020, VOT2021, and VOT2022bbox [11, 13, 12]. These sequences feature multiple objects and many occlusions, which are the scenarios we wish to address. The NeighborTrack algorithm can be used with various S-networks, such as Ocean [33], TransT [5] and OSTrack [31], to effectively overcome appearance changes and occlusions. In addition, we use the mainstream medium and long-term datasets of the SOT field, including LaSOT [8] and GOT-10K [10], to verify NeighborTrack with the state-of-the-art method, OSTrack [31]. VOT2020 and VOT2021 are mask datasets, while LaSOT, VOT2022bbox, and GOT-10K are bbox datasets. We apply NeighborTrack to three previous models: a traditional attention-based network Ocean [33], a transformer-based network TransT [5], and a state-of-the-art network OSTrack [31].

4.3 VOT datasets

Several quantitative metrics are provided in the annual VOT challenge [13] for comparing the performance of SOT methods. The metrics include (1) accuracy: the average IoU between the tracker output and the ground truth before tracking failure, (2) robustness: the percentage of successfully tracked sub-sequence frames, (3) Expected Average Overlap (EAO): the expected value of IoU between each tracking result and the ground truth. For all metrics, higher is better. For accuracy, because we calculate the average IoU only when tracking is successful, we cannot determine whether the result is good or bad when tracking fails; the robustness metric, on the other hand, only reacts when tracking fails. Compared to these metrics, the EAO metric is a principled combination of tracking accuracy and robustness, thus providing a more comprehensive picture of whether tracking has been successful or not. Therefore, EAO has usually been used as the primary performance measure.

Table 1: The effect of changing τ on the calculation speed/AUC: Take for example the experiments on NeighborTrack on LaSOT benchmark[8] using OSTrack as the basis. From the table, we can see that the frame rate decays as τ increases. In addition, the tracking effect is slightly reduced if Kalman filter is not introduced, but at the same time, the frame rate is slightly improved.

model name	AUC↑	LaSOT FPS(Hz)↑
OSTrack384[31]	0.711	3.63
OSTrack384[31]+ours τ =3	0.714	2.40
OSTrack384[31]+ours τ =9	0.722	1.58
OSTrack384[31]+ours w/o Kalman filter τ =9	0.720	1.71
OSTrack384[31]+ours τ =27	0.720	0.75
OSTrack384[31]+ours τ =36	0.721	0.6

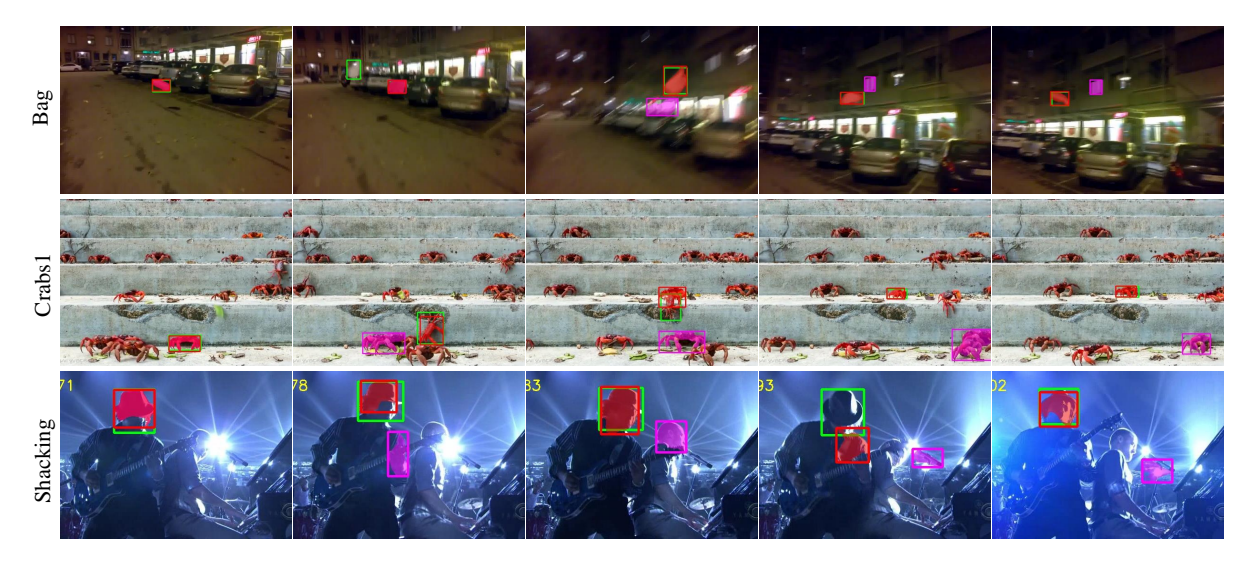


Figure 4: Examples of tracking results with and without NeighborTrack from VOT [13]. We use TransT [5] as a baseline and correct its results using NeighborTrack. Ground truth is indicated by the green boxes. Magenta boxes and masks represent baseline results, while red boxes and masks represent results after applying NeighborTrack. Bag and Crabs1 are examples that the baseline is unable to track because there are other objects that resemble the target. In the case of shacking, occlusion and deformation cause severe appearance changes, leading to the failure of the baseline. In most cases, tracking errors are corrected after NeighborTrack has been applied.

Table 2: Results of applying NeighborTrack to three different SOT methods on the VOT benchmarks [13]. Green numbers indicate that the original model has been improved.

	VOT2020			
model name	accuracy↑ robustness↑		EAO↑	
Ocean[33]+AR[30]	0.757 0.810		0.515	
Ocean[33]+AR[30] +ours	0.755 0.807		0.516	
TransT[5]+AR[30]	0.769 0.775		0.490	
TransT[5]+AR[30] + ours	0.768 0.816		0.523	
OSTrack[31]+AR[30]	0.770 0.812		0.526	
OSTrack[31]+AR[30] +ours	0.769 0.844		0.553	
	VOT2021			
Ocean[33]+AR[30]	0.756 0.803		0.510	
Ocean[33]+AR[30] +ours	0.754 0.803		0.515	
TransT[5]+AR[30]	0.768 0.775		0.494	
TransT[5]+AR[30] +ours	0.767 0.809		0.519	
OSTrack[31]+AR[30]	0.770 0.810		0.528	
OSTrack[31]+AR[30] +ours	0.769 0.843 0		0.556	
	VOT2022bbox			
Ocean[33]	0.703	0.823	0.484	
Ocean[33] +ours	0.703 0.822		0.486	
TransT[5]	0.780 0.775		0.493	
TransT[5] +ours	0.781	0.808	0.519	
OSTrack[31]	0.779	79 0.824 0		
OSTrack[31] +ours	0.779 0.845 0.564		0.564	
	Average			
+ours	-0.07%	+2.11%	+1.92%	



Figure 5: Examples of tracking results with and without NeighborTrack from LaSOT [8]. We apply NeighborTrack to correct the tracking results of OSTrack [31]. Ground truth is indicated by the green boxes. OSTrack's results are represented by magenta boxes, while NeighborTrack's results are represented by red boxes. OSTrack fails to track Bicycle-9 and Dog-1 due to the occlusion of the target, whereas it fails to track Flag-2 due to the target's deformation. NeighborTrack is able to correct the majority of tracking errors.

Table 2 shows the results of the proposed NeighborTrack. NeighborTrack is used to augment three representative models, Ocean, TransT, and OSTrack. Overall, NeighborTrack improves EAO by 1.92% and robustness by 2.11% on average. The accuracy decreases slightly at -0.07% because this metric only considers the average IoU of successful tracking, while the frames that fail to track do not participate in its calculation. In an extreme case, if the tracking fails in the second frame after the start, the accuracy calculation will reach the maximum of 1.0 since only the ground truth is used in the calculation process. However, this cannot be considered successful tracking. With our method, tracking will be less likely to be interrupted, but the detected bounding box position could be inaccurate if the target is obscured. The other two metrics, robustness and EAO, demonstrate that our method has the ability to help SOT models track the target more consistently and effectively. In particular, for the primary metric EAO, NeighborTrack improves all three models on all datasets. The results show that our method is agnostic and effective to different types of SOT models.

Figure 4 illustrates the tracking results for some examples. In the figure, the green box represents the ground truth; the magenta box represents the original results of the baseline, TransT [5]; and the red box represents the NeighborTrack-corrected results. In the Bag example, since the garbage bag is white, as is the license plate and window, a tracker is likely to be confused. After applying NeighborTrack, although there will still be a small amount of false tracking, tracking can be resumed very quickly in contrast to TransT, which cannot be resumed after losing track. Crabs1 is a more challenging example since the crabs have similar appearances, which can lead to false tracking when they are close to each other. By introducing a mechanism of utilizing neighbors, our proposed method effectively reduces thetracking failure caused by appearance similarity. As a final example, we examine Shacking, an example with a singer shacking. TransT loses tracks as a result of being attracted to other objects, such as the arm, other people's heads, and finally the drum. Our method briefly mistracks when the face is completely obscured by the hat, but returns to the correct position as soon as the face appears again.

4.4 LaSOT and GOT-10K datasets

For the experiments of medium-term and long-term tracking, we used two datasets, LaSOT [8] and GOT-10K [10]. We use the metrics suggested by each dataset. Table 3 summarizes the results. The top three results are colored red, green, and blue, respectively. For LaSOT, OSTrack384 [31] leads all other methods. When NeighborTrack is applied to OSTrack384, its performance is further improved, and OSTrack384+NeighborTrack outperforms all other methods in all metrics. The performance of OSTrack384 on GOT-10K is substantially inferior to MixFormer-L [6], the best method excluding ours. OSTrack384+NeighborTrack, however, outperforms MixFormer-L, because NeighborTrack boosts OSTrack384 significantly. Accordingly, NeighborTrack achieves state-of-the-art results for both the LaSOT and GOT-10K datasets.

Table 3: Comparisons of NeighborTrack (applied to OSTrack384) and other leading methods on the LaSOT [8] and GOT-10K [10] datasets.

model name	AUC↑	LaSOT Norm-Precision↑	Precision [†]	
OSTrack384[31] +ours	0.722	0.818	0.780	
OSTrack384[31]	0.711	0.811	0.776	
SwinV2-L 1K-MIM[26]	0.707	_	_	
SwinTrack-B-384[17]	0.702	0.784	0.753	
MixFormer-L[6]	0.701	0.799	0.763	
AiATrack[9]	0.690	0.794	0.738	
Unicorn[28]	0.685	0.766	0.741	
KeepTrack[20]	0.671	0.772	0.702	
DMTrack[34]	0.574	_	0.580	
	GOT-10K			
model name	AO↑	$SR_{0.5} \uparrow$	$SR_{0.75} \uparrow$	
OSTrack384[31] +ours	0.757	0.8572	0.733	
MixFormer-L[6]	0.756	0.8573	0.728	
OSTrack384[31]	0.737	0.832	0.708	
SwinV2-L 1K-MIM[26]	0.729	_	_	
SwinTrack-B-384 [17]	0.724	0.805	0.678	
AiATrack[9]	0.696	0.800	0.632	
STARK[29]	0.688	0.781	0.641	

Figure 5 provides examples of tracking results for LaSOT. In Bicycle-9, a bicycle is tracked as it travels in an array of vehicles. When a white car obscures the bicycle, the tracker tracks a similar-looking black motorcycle, since it loses its target. NeighborTrack recognizes that the black motorcycle is not the intended target, so it is set up to re-track the target at a later time. Our method has succeeded in this example by introducing the Kalman filter, which provides candidates independent of appearance features, thus providing a greater range of options to the tracking system. Although the Kalman filter is not extremely accurate, it can serve as a guide to prevent the tracker from becoming outrageous. Dog-1 involves tracking a dog. When the dog is obscured by a tree, the tracker mistakenly selects the remote control car as the target. NeighborTrack detected a wrong target and switched to a near-blocker object framed by a Kalman filter-generated box. Flag-2 shows a typical example of appearance change due to deformation. In this case, the target to be tracked is a towed flag whose appearance varies greatly over time because of the soft nature of the flag and its variable pattern. Traditional methods can cause confusion between the flag and the parachute adjacent to it. Using NeighborTrack, as long as one of the two sides is relatively stable, neighbor information should be useful in reducing tracking failures caused by such deformation.

5 Conclusion

We propose NeighborTrack, a post-processing scheme that is agnostic and can be applied to state-of-the-art single object tracking methods provided that confidence scores are available. Through the use of neighbor information, NeighborTrack effectively mitigates the appearance change problem caused by occlusion or deformation. Our approach can be applied to both non-transformer-based methods [33] and transformer-based methods [5, 31]. Extensive experiments demonstrate that the proposed method is capable of improving the tracking performance of various SOT methods. There is no need to collect any additional training data for the proposed method. Furthermore, there is no need to retrain the SOT network. In summary, NeighborTrack complements most current state-of-the-art SOT algorithms and improves their accuracy.

References

- [1] Amanda Berg, Joakim Johnander, Flavie Durand de Gevigney, Jorgen Ahlberg, and Michael Felsberg. Semi-automatic annotation of objects in visual-thermal video. In <u>Proceedings of the IEEE/CVF International Conference on Computer Vision</u> (ICCV) Workshops, Oct 2019. 1
- [2] Luca Bertinetto, Jack Valmadre, João F. Henriques, Andrea Vedaldi, and Philip H. S. Torr. Fully-convolutional siamese networks for object tracking. In Gang Hua and Hervé Jégou, editors, <u>Computer Vision ECCV 2016 Workshops</u>, pages 850–865, Cham, 2016. 1, 3
- [3] Goutam Bhat, Martin Danelljan, Luc Van Gool, and Radu Timofte. Learning discriminative model prediction for tracking. In 2019 IEEE/CVF International Conference on Computer Vision (ICCV), pages 6181–6190, 2019. 2, 3

- [4] Navaneeth Bodla, Bharat Singh, Rama Chellappa, and Larry S. Davis. Soft-NMS improving object detection with one line of code, 2017. 5, 7
- [5] Xin Chen, Bin Yan, Jiawen Zhu, Dong Wang, Xiaoyun Yang, and Huchuan Lu. Transformer tracking. In Proceedings of the IEEE/CVF Conference on Computer Vision and Pattern Recognition (CVPR), pages 8126–8135, June 2021. 3, 7, 8, 9, 10
- [6] Yutao Cui, Cheng Jiang, Limin Wang, and Gangshan Wu. Mixformer: End-to-end tracking with iterative mixed attention. In Proceedings of the IEEE/CVF Conference on Computer Vision and Pattern Recognition (CVPR), pages 13608–13618, June 2022. 3, 9, 10
- [7] Weijian Deng, Liang Zheng, Qixiang Ye, Guoliang Kang, Yi Yang, and Jianbin Jiao. Image-image domain adaptation with preserved self-similarity and domain-dissimilarity for person re-identification. In Proc. CVPR, 2018. 3
- [8] Heng Fan, Liting Lin, Fan Yang, Peng Chu, Ge Deng, Sijia Yu, Hexin Bai, Yong Xu, Chunyuan Liao, and Haibin Ling. Lasot: A high-quality benchmark for large-scale single object tracking. In Proceedings of the IEEE/CVF Conference on Computer Vision and Pattern Recognition (CVPR), June 2019. 3, 4, 7, 9, 10
- [9] Shenyuan Gao, Chunluan Zhou, Chao Ma, Xinggang Wang, and Junsong Yuan. AiATrack: Attention in attention for transformer visual tracking. In European Conference on Computer Vision, pages 146–164. Springer, 2022. 10
- [10] Lianghua Huang, Xin Zhao, and Kaiqi Huang. Got-10k: A large high-diversity benchmark for generic object tracking in the wild. IEEE Transactions on Pattern Analysis and Machine Intelligence, 43(5):1562–1577, 2021. 3, 7, 9, 10
- [11] Matej Kristan, Alan Lukezi c, Martin Danelljan, Luka Cehovin Zajc, and Jiri Matas. The new VOT2020 short-term tracking performance evaluation protocol and measures, 2020.
- [12] Matej Kristan, JiriMatas, Aleš Leonardis, Michael Felsberg, Roman Pflugfelder, Joni-Kristian Kamarainen, Hyung Jin Chang, Martin Danelljan, Luka Čehovin Zajc, Alan Lukežič, Ondrej Drbohlav, Jani Kapyla, Gustav Hager, Song Yan, Jinyu Yang, Zhongqun Zhang, Gustavo Fernandez, and et. al. The ninth visual object tracking VOT2021 challenge results, 2021.
- [13] Matej Kristan, Jiri Matas, Aleš Leonardis, Tomas Vojir, Roman Pflugfelder, Gustavo Fernandez, Georg Nebehay, Fatih Porikli, and Luka Čehovin. A novel performance evaluation methodology for single-target trackers. IEEE Transactions on Pattern Analysis and Machine Intelligence, 38(11):2137–2155, Nov 2016. 3, 7, 8
- [14] B Y Lee, L H Liew, W S Cheah, and Y C Wang. Occlusion handling in videos object tracking: A survey. <u>IOP Conference</u> Series: Earth and Environmental Science, 18:012020, feb 2014. 3
- [15] Bo Li, Wei Wu, Qiang Wang, Fangyi Zhang, Junliang Xing, and Junjie Yan. SiamRPN++: Evolution of siamese visual tracking with very deep networks. In <u>Proceedings of the IEEE/CVF Conference on Computer Vision and Pattern Recognition (CVPR)</u>, June 2019. 3
- [16] Bo Li, Junjie Yan, Wei Wu, Zheng Zhu, and Xiaolin Hu. High performance visual tracking with siamese region proposal network. In 2018 IEEE/CVF Conference on Computer Vision and Pattern Recognition, pages 8971–8980, 2018.
- [17] Liting Lin, Heng Fan, Yong Xu, and Haibin Ling. Swintrack: A simple and strong baseline for transformer tracking. <u>arXiv</u> preprint arXiv:2112.00995, 2021. 10
- [18] Liwei Liu, Junliang Xing, Haizhou Ai, and Xiang Ruan. Hand posture recognition using finger geometric feature. In Proceedings of the 21st International Conference on Pattern Recognition (ICPR2012), pages 565–568, 2012.
- [19] Akshay Mangawati, Mohana, Mohammed Leesan, and H. V. Ravish Aradhya. Object tracking algorithms for video surveillance applications. In 2018 International Conference on Communication and Signal Processing (ICCSP), pages 0667–0671, 2018.
- [20] Christoph Mayer, Martin Danelljan, Danda Pani Paudel, and Luc Van Gool. Learning target candidate association to keep track of what not to track. In <u>Proceedings of the IEEE/CVF International Conference on Computer Vision</u>, pages 13444–13454, 2021. 3, 10
- [21] A. Milan, L. Leal-Taixé, I. Reid, S. Roth, and K. Schindler. MOT16: A benchmark for multi-object tracking. arXiv:1603.00831 [cs], Mar. 2016. arXiv: 1603.00831. 2, 6
- [22] J. Munkres. Algorithms for the assignment and transportation problems. <u>Journal of the Society of Industrial and Applied Mathematics</u>, 5(1):32–38, March 1957. 6
- [23] Shaoqing Ren, Kaiming He, Ross Girshick, and Jian Sun. Faster R-CNN: Towards real-time object detection with region proposal networks. In <u>Advances in Neural Information Processing Systems</u>, volume 28, 2015. 3
- [24] Qiang Wang, Li Zhang, Luca Bertinetto, Weiming Hu, and Philip HS Torr. Fast online object tracking and segmentation: A unifying approach. In <u>Proceedings of the IEEE conference on computer vision and pattern recognition</u>, 2019. 1, 3
- [25] Xiaolong Wang, Allan Jabri, and Alexei A. Efros. Learning correspondence from the cycle-consistency of time. In <u>CVPR</u>, 2019. 4
- [26] Zhenda Xie, Zigang Geng, Jingcheng Hu, Zheng Zhang, Han Hu, and Yue Cao. Revealing the dark secrets of masked image modeling, 2022. 10
- [27] Junliang Xing, Haizhou Ai, and Shihong Lao. Multiple human tracking based on multi-view upper-body detection and discriminative learning. In 2010 20th International Conference on Pattern Recognition, pages 1698–1701, 2010.
- [28] Bin Yan, Yi Jiang, Peize Sun, Dong Wang, Zehuan Yuan, Ping Luo, and Huchuan Lu. Towards grand unification of object tracking. In European Conference on Computer Vision(ECCV), 2022. 10
- [29] Bin Yan, Houwen Peng, Jianlong Fu, Dong Wang, and Huchuan Lu. Learning spatio-temporal transformer for visual tracking. In Proceedings of the IEEE/CVF International Conference on Computer Vision, pages 10448–10457, 2021. 10
- [30] Bin Yan, Xinyu Zhang, Dong Wang, Huchuan Lu, and Xiaoyun Yang. Alpha-refine: Boosting tracking performance by precise bounding box estimation. In IEEE Conference on Computer Vision and Pattern Recognition, CVPR 2021, virtual, June 19-25, 2021, pages 5289–5298. Computer Vision Foundation / IEEE, 2021. 2, 8

- [31] Botao Ye, Hong Chang, Bingpeng Ma, and Shiguang Shan. Joint feature learning and relation modeling for tracking: A one-stream framework. In European Conference on Computer Vision(ECCV), 2022. 3, 4, 7, 8, 9, 10
- [32] Yifu Zhang, Chunyu Wang, Xinggang Wang, Wenjun Zeng, and Wenyu Liu. Fairmot: On the fairness of detection and re-identification in multiple object tracking. International Journal of Computer Vision (to appear), August 2021. 3
- [33] Zhipeng Zhang, Houwen Peng, Jianlong Fu, Bing Li, and Weiming Hu. Ocean: Object-aware anchor-free tracking. In Computer Vision - ECCV 2020 - 16th European Conference, Glasgow, UK, August 23-28, 2020, Proceedings, Part XXI, volume 12366 of Lecture Notes in Computer Science, pages 771–787. Springer, 2020. 3, 7, 8, 10
- [34] Zikai Zhang, Bineng Zhong, Shengping Zhang, Zhenjun Tang, Xin Liu, and Zhaoxiang Zhang. Distractor-aware fast tracking via dynamic convolutions and mot philosophy. In Proceedings of the IEEE/CVF Conference on Computer Vision and Pattern Recognition (CVPR), pages 1024–1033, June 2021. 3, 10